

Dual Oxidase/ Oxygenase Reactivity and Resonance Raman Spectrum of {Cu₃O₂} Moiety with Perfluoro-t-butoxide Ligands

Sarah E.N. Brazeau, Emily E. Norwine, Steven F. Hannigan, Nicole Orth, Ivana Ivanović-Burmazović, Dieter Rukser, Florian Biebl, Benjamin Grimm-Lebsanft, Gregor Praedel, Melissa Teubner, Michael Rübhausen, Patricia Liebhäuser, Thomas Rösener, Julia Stanek, Alexander Hoffmann, Sonja Herres-Pawlis, and Linda H. Doerr

Supporting Information

Item	Title	Page
Figure S1	Resonance Raman of T _{OC4F9} at different wavelengths	2
Figure S2	DFT-optimized singlet for T _{OC4F9} .	3
Figure S3	UV-vis spectra of fully-formed T _{OC4F9} at different concentrations after 375 s.	3
Figure S4a	Absorbance at $\lambda = 520$ nm vs. time for seven different Cu concentrations for 75 s.	4
Figure S4b	Experimental vs. fit of absorbance $\lambda = 520$ nm vs. time for [Cu]= 4.95 mM at 75 s.	4
	Method for analysis of absorbance vs. time data	5
Figure S5	Absorbance vs. time data for 4.95 mM at 7.5 s before and after dip removal.	5
Figure S6	Absorbance at $\lambda = 520$ nm of {Cu ₃ O ₂ } ³⁻ from 5 mM initial Cu(I) at -78 °C in THF over 219 minutes.	6
Figure S7a	Representative ¹ H NMR spectrum showing catalytic H ₂ Q to BQ conversion in d ⁶ -acetone, inset on aromatic region.	7
Figure S7b	Representative ¹ H NMR spectrum showing catalytic H ₂ Q to BQ conversion in d ⁶ -acetone, full spectrum.	8
Figure S8a	Representative ¹ H NMR spectrum of run #10 showing catechol Product A formation, inset.	9
Figure S8b	Representative ¹ H NMR spectrum of run #10 showing catechol Product B formation, full spectrum.	10
Figure S8c	Representative ¹ H NMR spectrum of run #16 showing catechol Product B formation.	11
Figure S9	Identification of unlabeled (¹⁶ O) catechol by DART+ MS.	12
Figure S10	Identification of isotopically labeled (¹⁸ O) catechol by ¹ H NMR.	13
Figure S11	Identification of isotopically labeled (¹⁸ O) catechol by DART+ MS.	13
Table S1	Summary of <i>k_f</i> values for two-step model (A → B → C).	14-15
Table S2	Summary of <i>k_f</i> values for 4.95 mM at 520 nm, for one step model (A → B).	15
Table S3	Summary of <i>k_f</i> values for two concentrations for two-step model (A → B → C) and the standard deviation for the residuals σ_r (global analysis).	16
Table S4	Summary of <i>k_f</i> values for two concentrations for global analysis and the standard deviation for the residuals σ_r , for one step model (A → B).	16
Table S5	Catalytic H ₂ Q oxidation to BQ by T _{OC4F9} in THF at -78°C.	17
Table S6	Product quantification in hydroxylation of phenolate (DBP) to catechol (DBC) by T _{OC4F9} in THF at -78°C	18

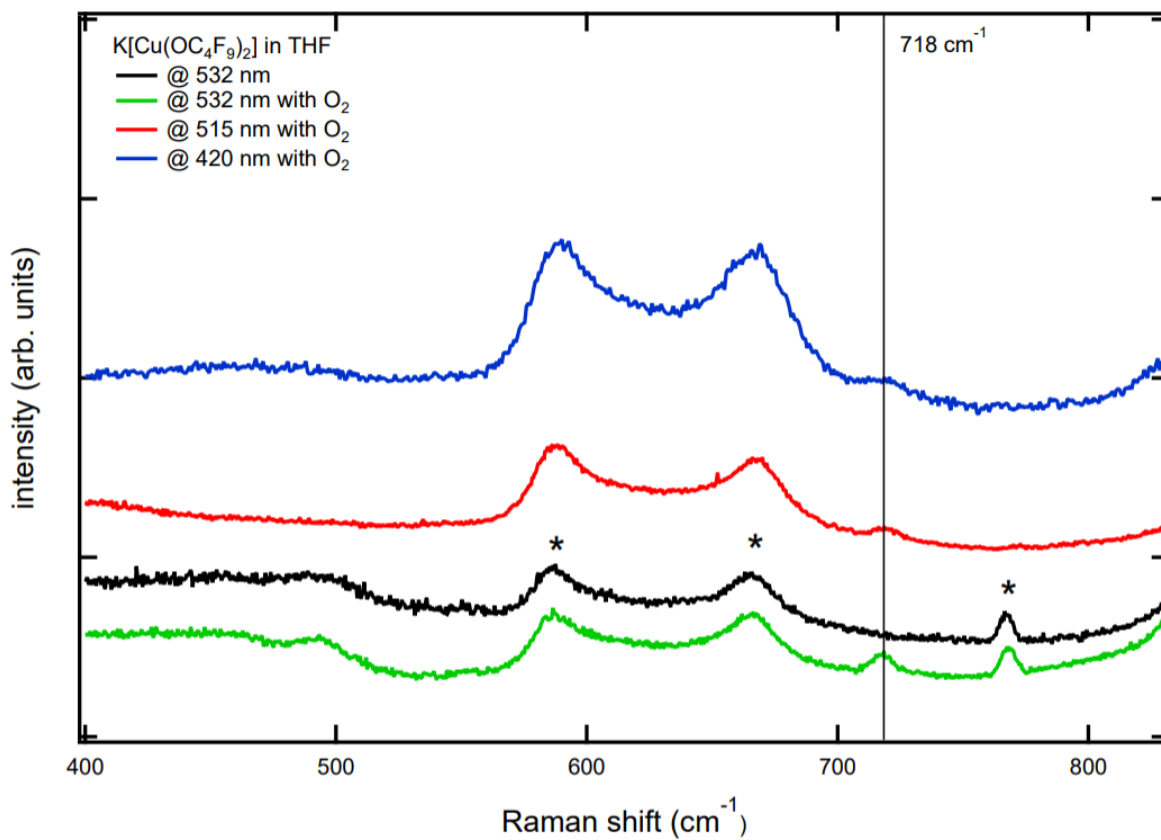


Figure S1. Resonance Raman of T_{OC₄F₉} at different wavelengths.

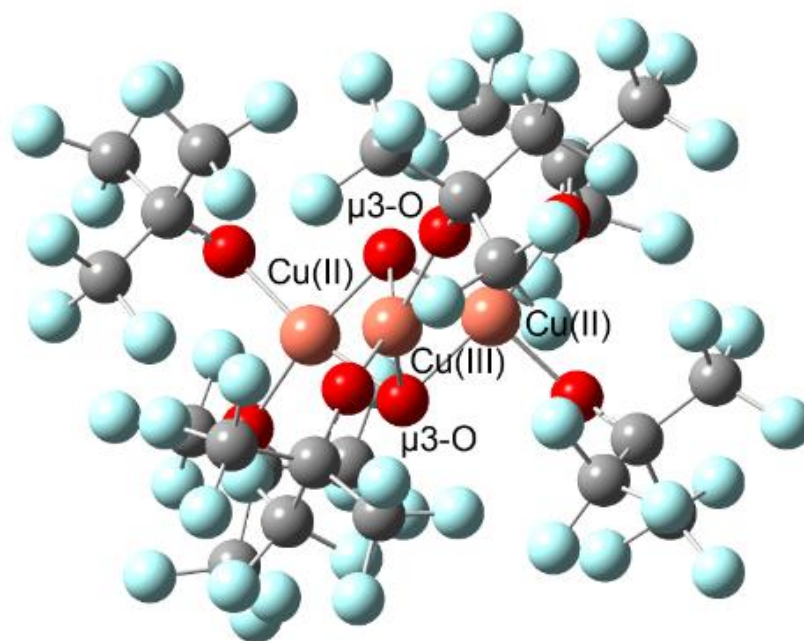


Figure S2. DFT-optimized $S = 0$ for SyToc4F9 .

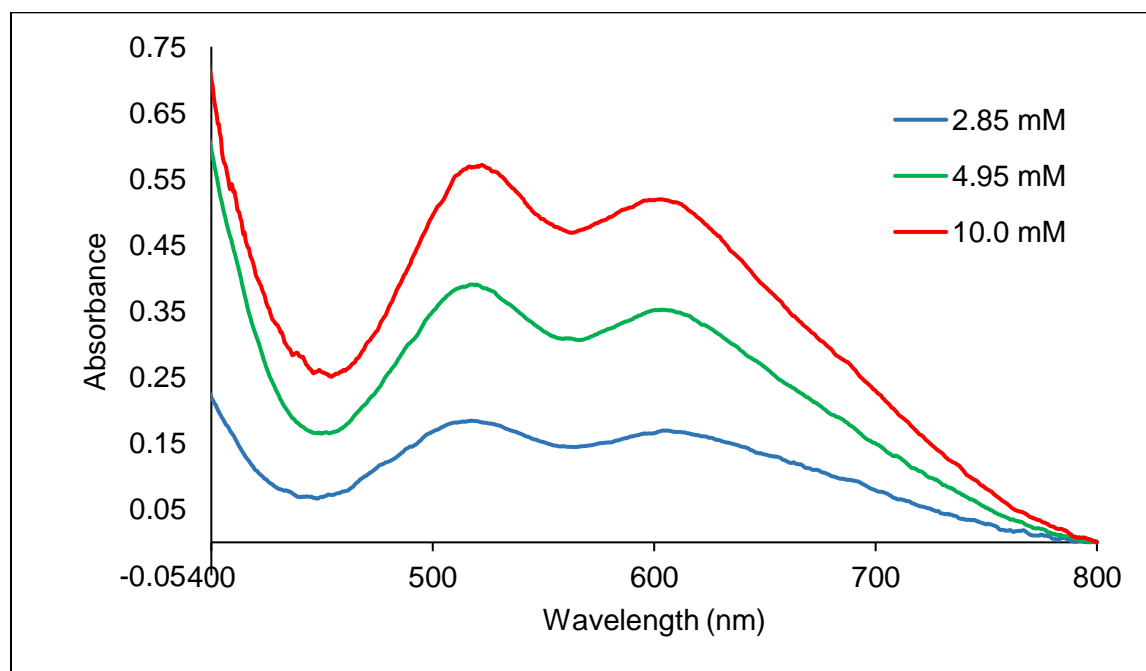


Figure S3. UV-vis spectra of fully-formed T_{OC4F9} at different concentrations after 375 s.

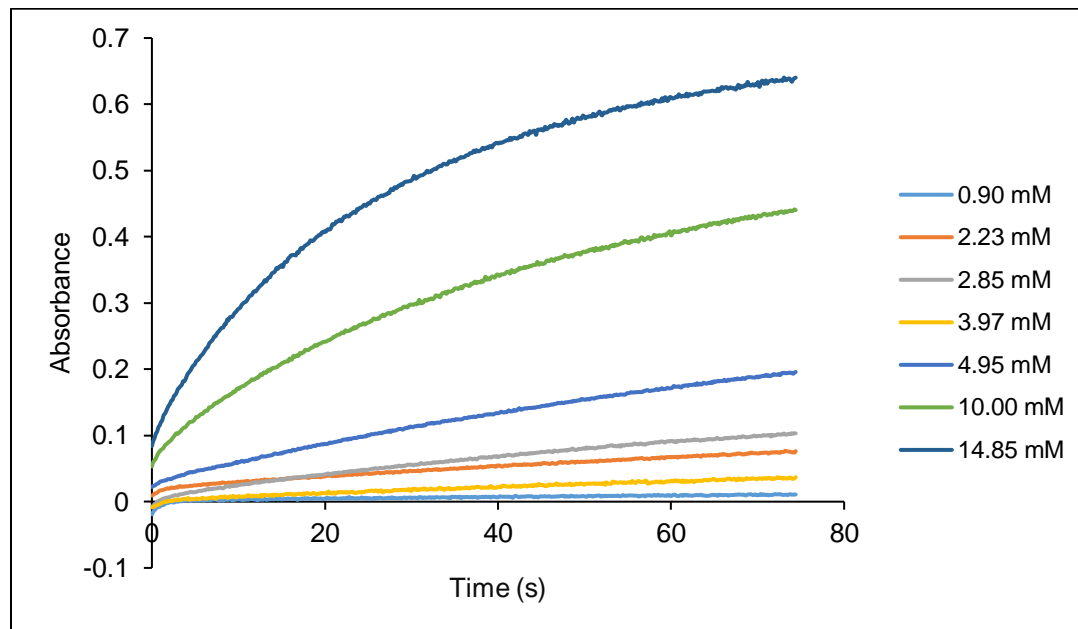


Figure S4a. Absorbance at $\lambda = 520$ nm vs. time for seven different Cu concentrations for 75 s.

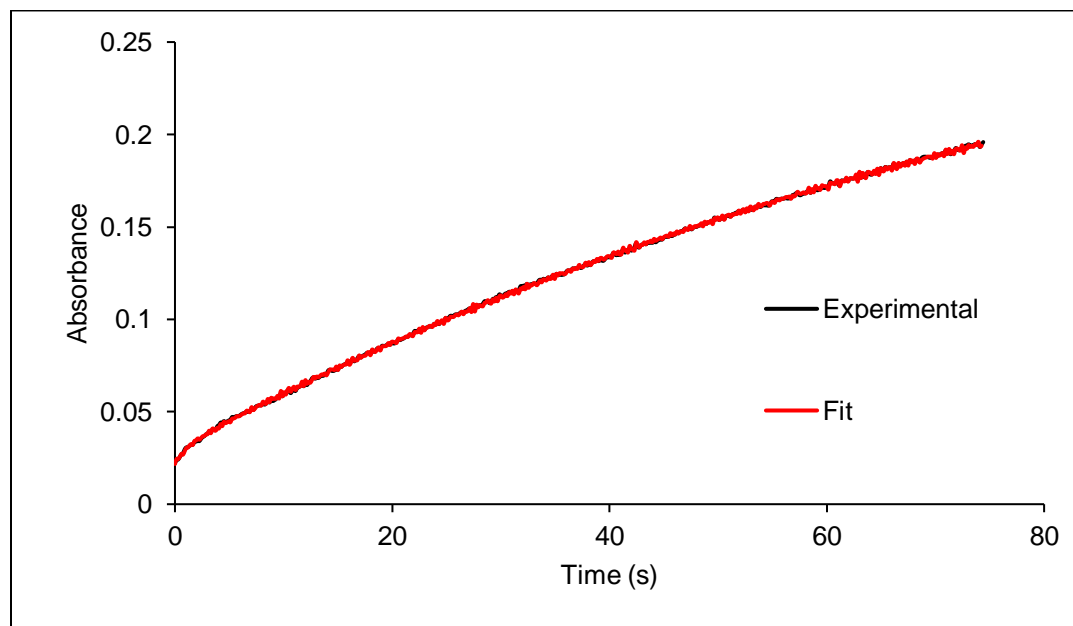


Figure S4b. Experimental vs. fit of absorbance $\lambda = 520$ nm vs. time for $[Cu] = 4.95$ mM at 75 s.

Method for analysis of absorbance vs. time data: All stopped flow experiments were performed using a HI-TECH Scientific SF-61SX2 device with a diode array and photomultiplier detector, with the TgK Scientific Program Kinetic Studio 4.0.8.18533. Analysis revealed the presence of only two visible peaks, 520 nm and 602 nm, that slowly grow in as T_{OC4F9} forms. Absorbance vs. time data were extracted from these files at 520 nm only, as kinetic behavior at both wavelengths was the same. When data from the shortest time stamps were plotted, a dip appears that results from the change in pressure as the solutions from the syringes are mixed. This dip interfered with the determination of steps and formation constants in the formation of T_{OC4F9} . The dip was removed by first eliminating only the x-values associated with this phenomenon, and then all x-values were subtracted from the first remaining x-value to shift the values to start at zero. The results of this procedure are shown in Figures S4 and S5. For larger time stamps (greater than 150 s), this modification was not necessary, as the dip was minimal. The resulting data were then imported into JPlus Consulting program ReactLab KINETICS (Build 10, Version 1.1). At all published concentrations, two steps were identified ($A \rightarrow B \rightarrow C$), believed to be first the formation of O_{OC4F9} , followed by the formation of T_{OC4F9} . Formation constants were determined for each process, with the results averaged together and presented in Tables 2 and 3 in this publication, with further details in Table S1 and Table S3. A one-step fit was also attempted (Table S2 and Table S4), but was unable to be fit.

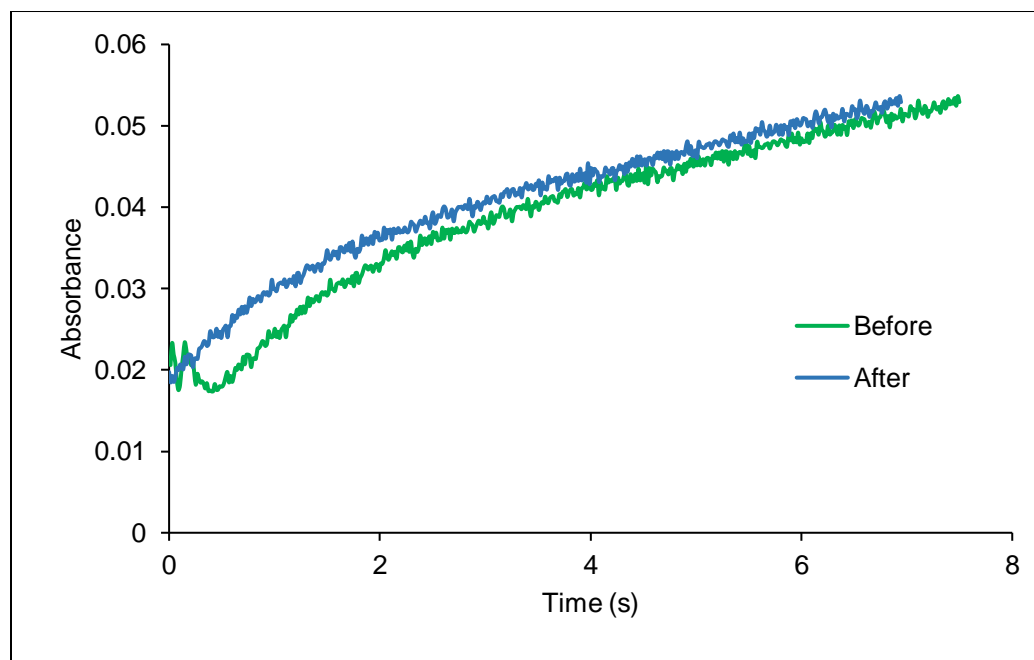


Figure S5. Absorbance at $\lambda = 520$ nm vs. time for $[Cu] = 4.95$ mM at 7.5 s before and after dip removal.

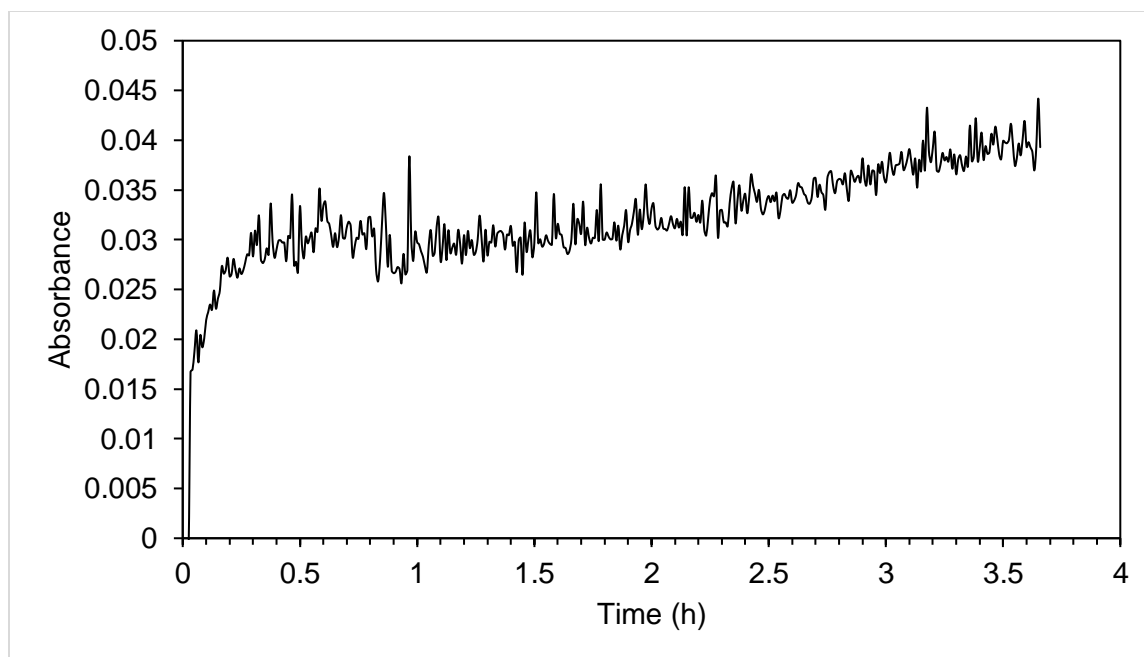


Figure S6. Absorbance at $\lambda = 520$ nm of $\{\text{Cu}_3\text{O}_2\}^{3-}$ from 5 mM initial Cu(I) at -78 °C in THF over 219 minutes.

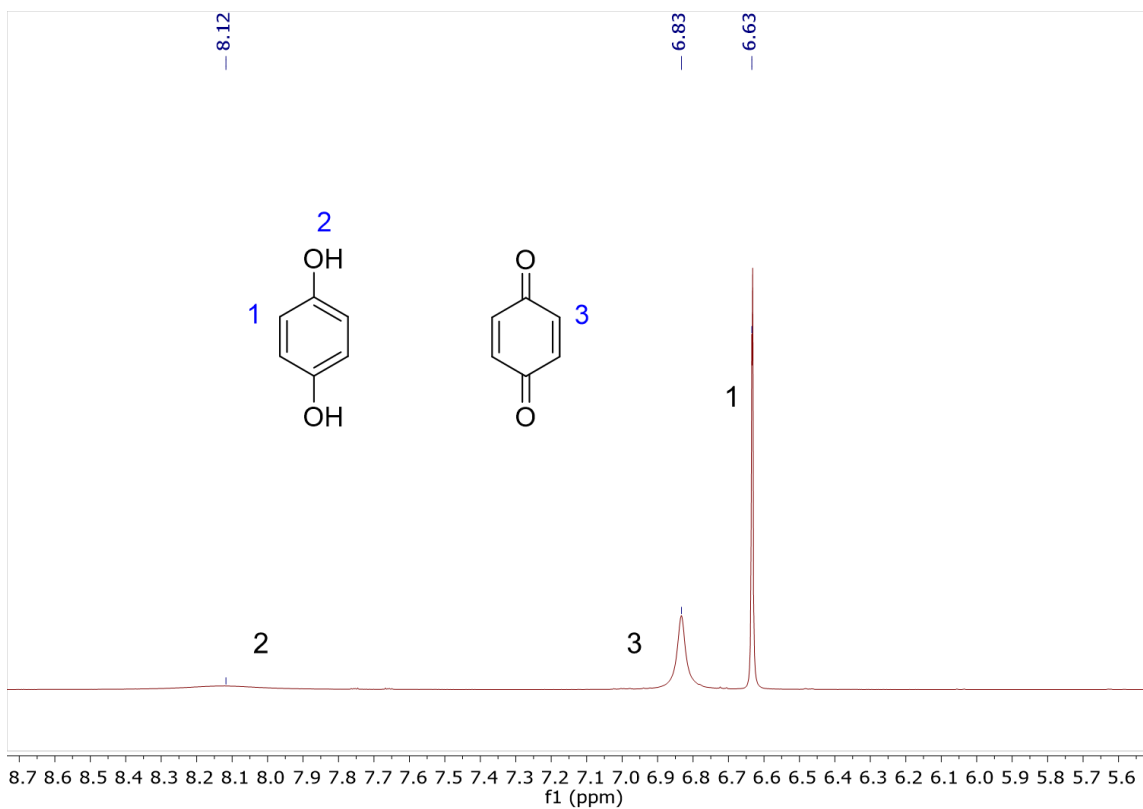


Figure S7a. ^1H NMR spectrum from the 5th run in Table S1 showing catalytic H₂Q to BQ conversion in d^6 -acetone, inset of full spectrum into aromatic region. ^1H NMR taken after reaction was warmed to room temperature and concentrated, with DMSO added as an internal standard. A relaxation delay of 5 seconds was used.

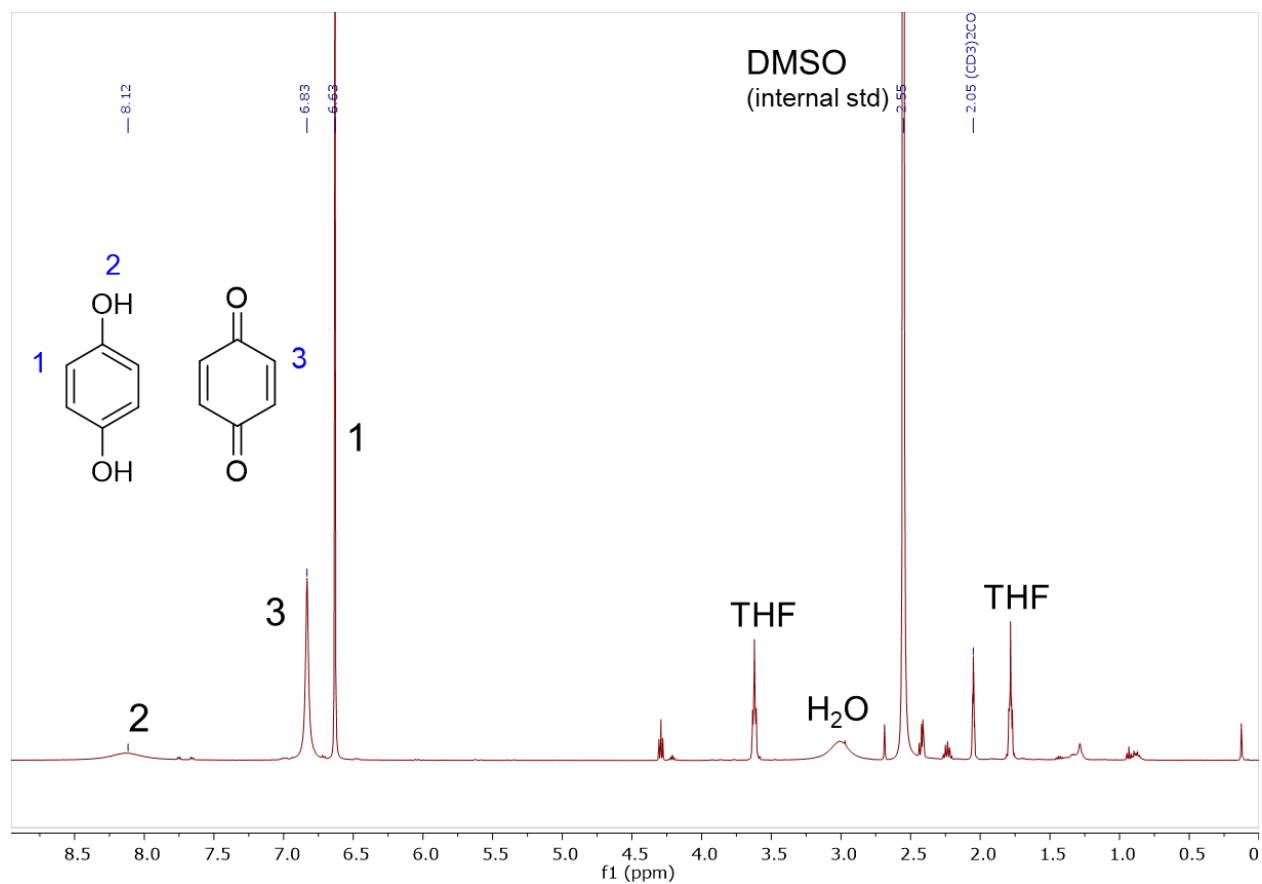


Figure S7b. Representative full ^1H NMR spectrum showing catalytic H_2Q to BQ conversion in d^6 -acetone. ^1H NMR taken after reaction was warmed to room temperature and concentrated, with DMSO added as an internal standard. A relaxation delay of 5 seconds was used.

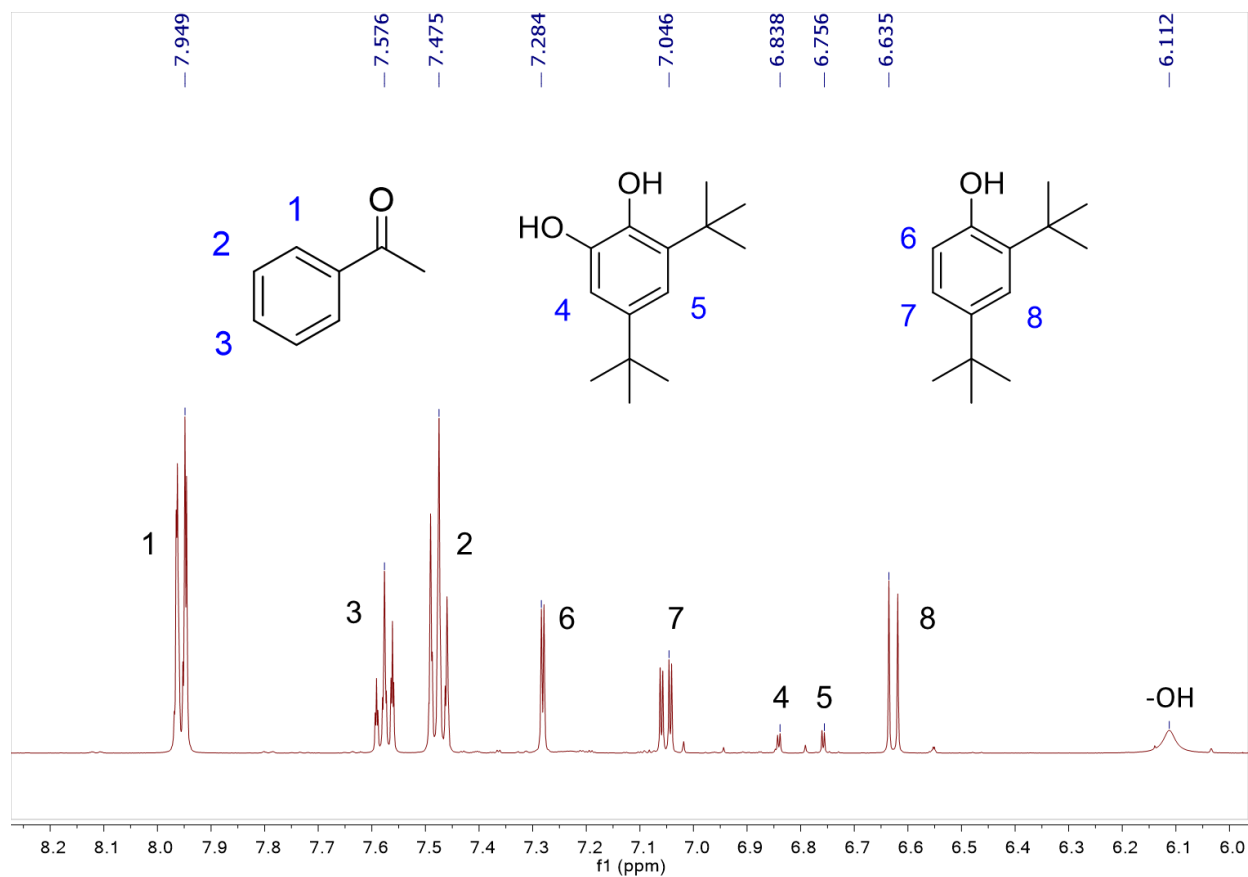


Figure S8a. Representative ^1H NMR spectrum of run #10 showing catechol product A formation in CD_2Cl_2 , zoom in on aromatic region. ^1H NMR taken after reaction was warmed to room temperature, quenched and extracted into organic solvent, with acetophenone added as an internal standard. A relaxation delay of 5 seconds was used.

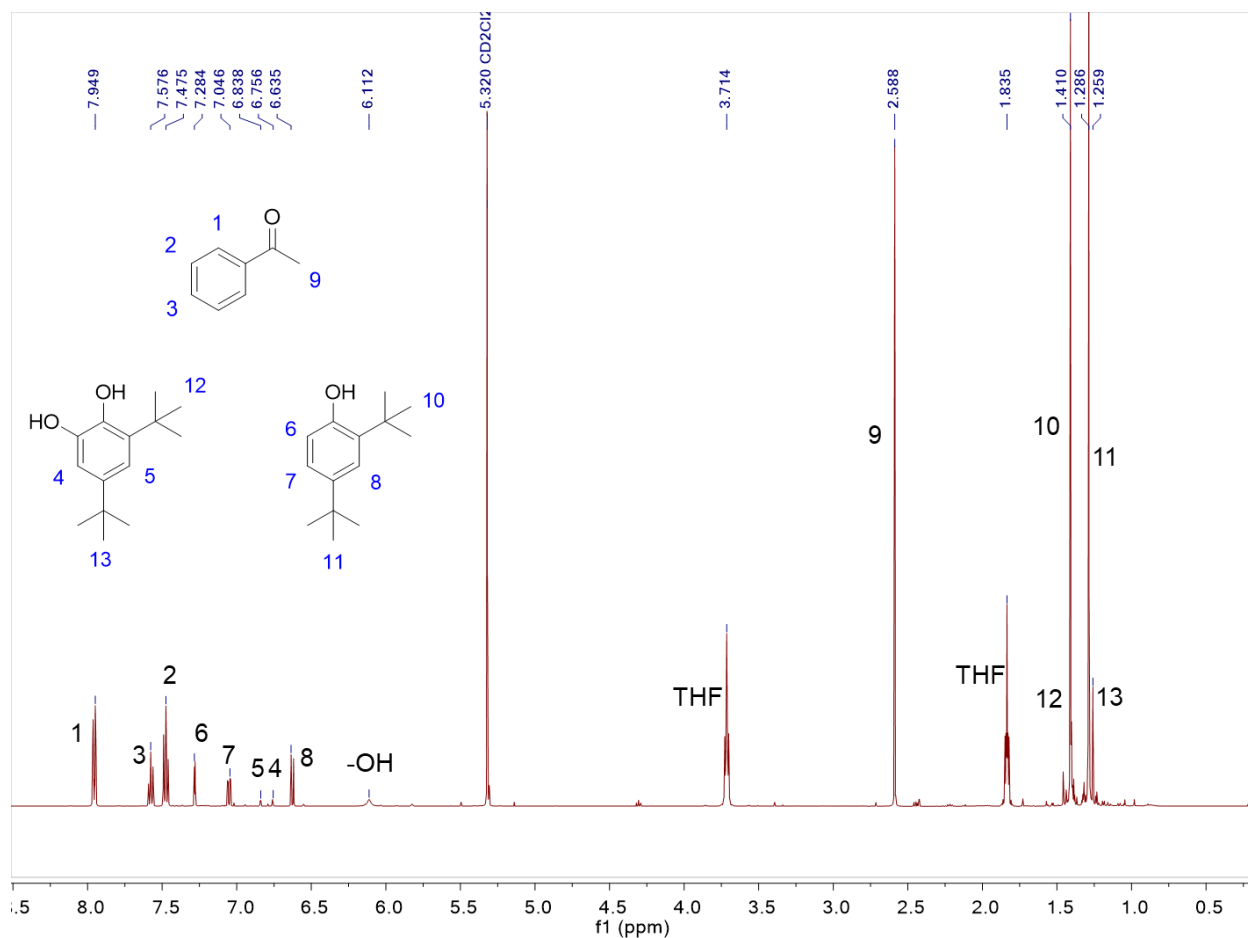


Figure S8b. Representative ¹H NMR spectrum of run #10 showing catechol product A formation in CD₂Cl₂, full spectrum of v1. ¹H NMR taken after reaction was warmed to room temperature, quenched and extracted into organic solvent, with acetophenone added as an internal standard. A relaxation delay of 5 seconds was used.

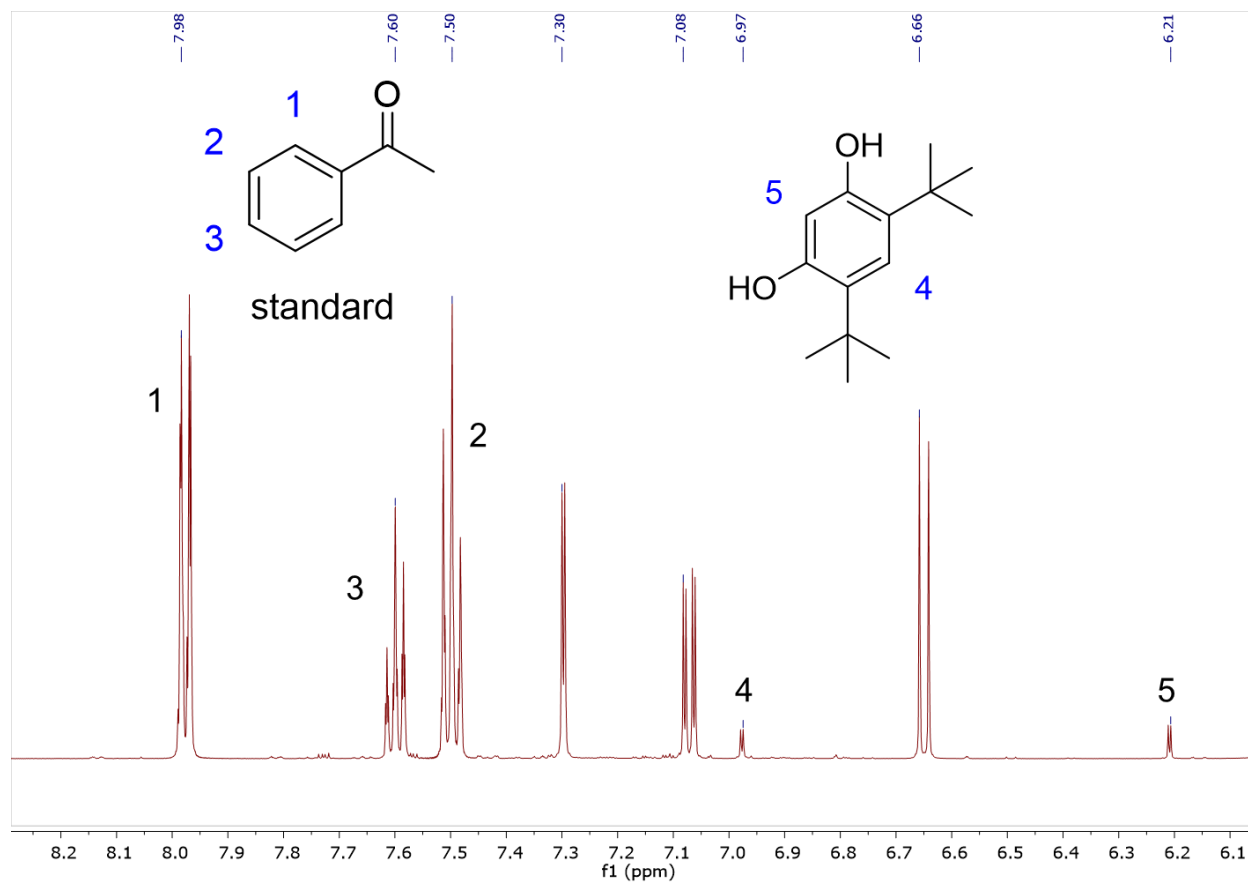


Figure S8c. Representative ^1H NMR spectrum of run #16 showing catechol product B formation in CD_2Cl_2 . ^1H NMR taken after reaction was warmed to room temperature, quenched and extracted into organic solvent, with acetophenone added as an internal standard. A relaxation delay of 5 seconds was used.

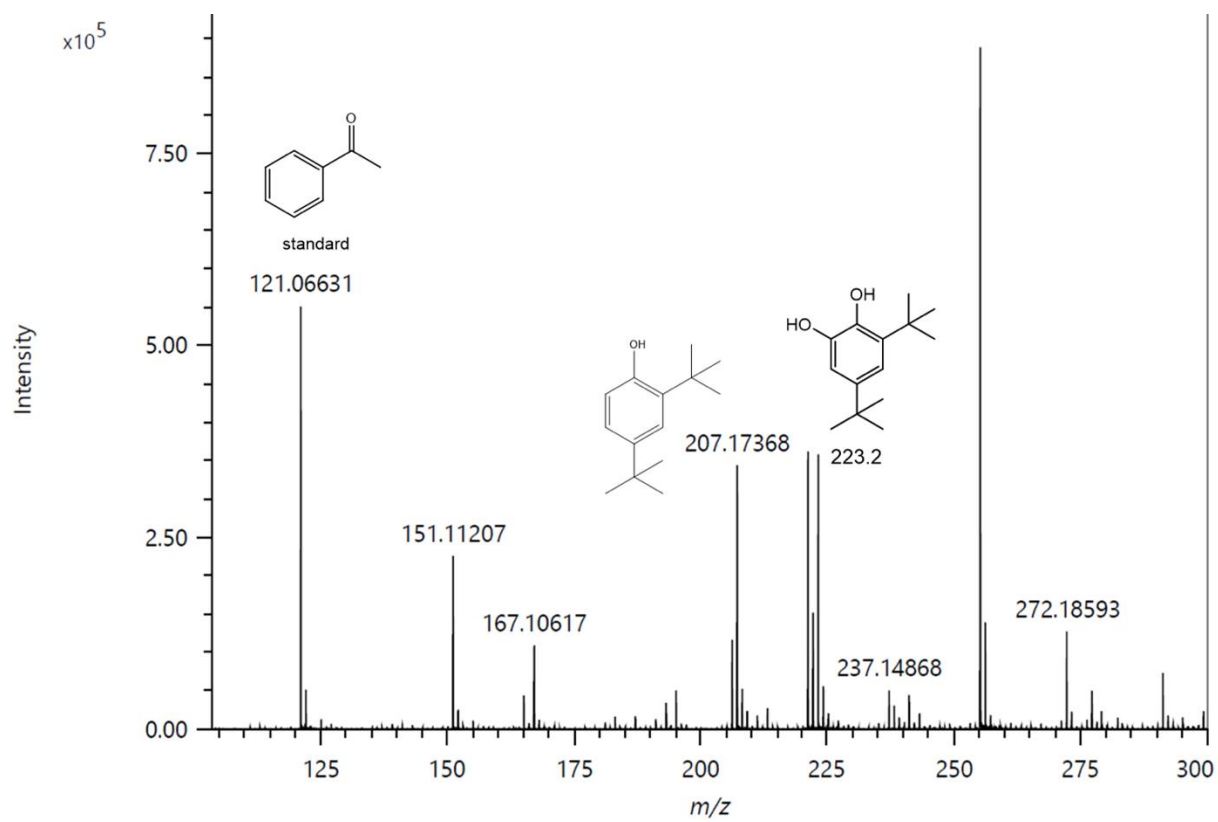


Figure S9. Identification of unlabeled (¹⁶O) catechol by DART+ MS.

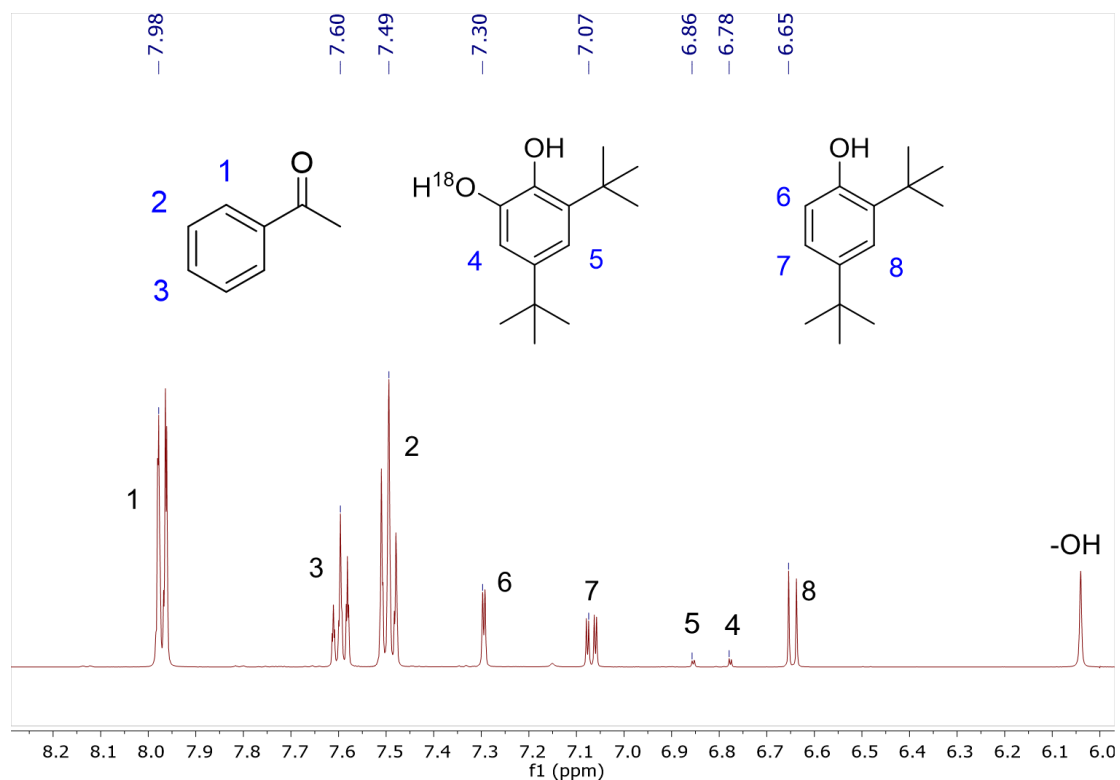


Figure S10. Identification of isotopically labeled (^{18}O) catechol by ^1H NMR. ^1H NMR taken after reaction was warmed to room temperature, quenched and extracted into organic solvent, with acetophenone added as an internal standard. A relaxation delay of 5 seconds was used.

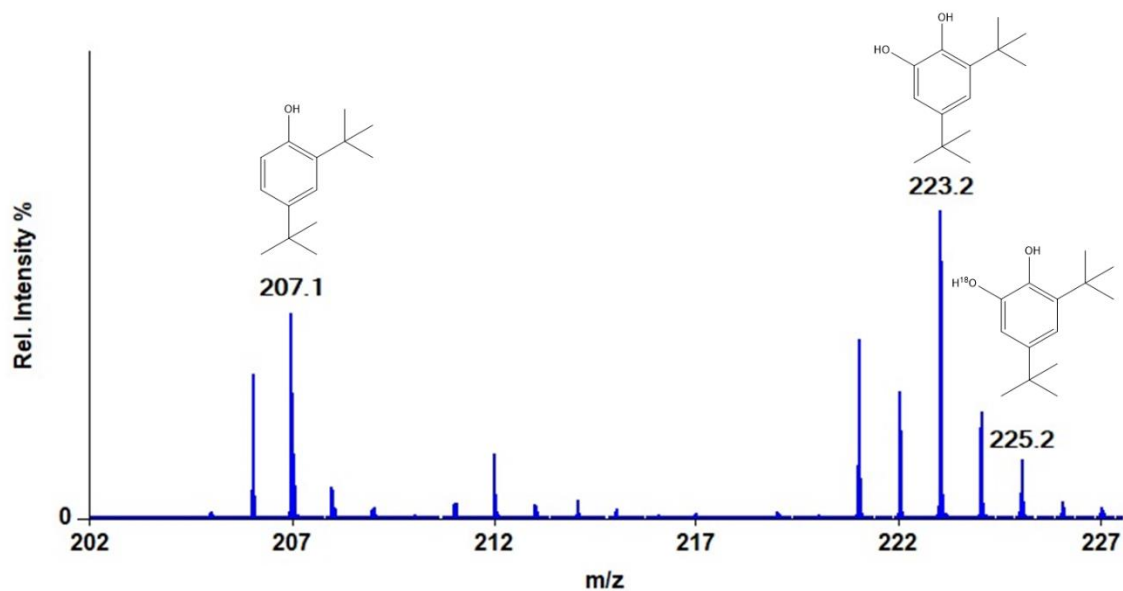


Figure S11. Identification of isotopically labeled (^{18}O) catechol by DART+ MS.

Table S1. Summary of k_f values for two-step model ($A \rightarrow B \rightarrow C$). For each Cu(I) concentration, several timestamps were evaluated by stopped flow. The absorbance vs. time data at 520 nm was then imported into ReactLab KINETICS, in which the data evaluated under pseudo first-order kinetics. This was found to fit to a two-step model, confirmed by a low residual. Greater detail can be found previously, in “Method for analysis of absorbance vs. time data.”

[Cu(I)] (mM)	Time (s)	k_{1-F} (s ⁻¹)	k_{2-F} (s ⁻¹)	Residual
0.9	7.5	1.16 ± 0.082	0.23 ± 0.10	0.0012
	15	1.08 ± 0.041	0.11 ± 0.030	0.0010
	75	0.84 ± 0.031	0.0097 ± 0.0011	0.0012
	150	0.87 ± 0.039	0.0041 ± 0.00031	0.0010
	750	0.45 ± 0.067	0.0031 ± 0.000035	0.0010
	Average	0.88 ± 0.052	0.071 ± 0.027	0.0011
2.23	7.5	1.02 ± 0.046	0.0046 ± 0.031	0.0011
	15	1.16 ± 0.078	0.072 ± 0.0085	0.0010
	37.5	0.99 ± 0.053	0.012 ± 0.0014	0.0013
	75	0.75 ± 0.045	0.0068 ± 0.00020	0.0012
	150	0.87 ± 0.082	0.0059 ± 0.000080	0.0018
	375	0.027 ± 0.0024	0.0041 ± 0.000075	0.0025
	Average	0.80 ± 0.051	0.018 ± 0.0070	0.0015
2.85	7.5	1.07 ± 0.10	0.010 ± 0.042	0.0020
	15	0.99 ± 0.046	0.018 ± 0.0041	0.0010
	75	0.67 ± 0.039	0.012 ± 0.00014	0.0015
	150	0.38 ± 0.024	0.010 ± 0.000056	0.0018
	750	0.029 ± 0.0014	0.0065 ± 0.00011	0.0020
	Average	0.63 ± 0.042	0.011 ± 0.0092	0.0017
3.97	7.5	1.35 ± 0.50	0.31 ± 0.098	0.0019
	15	0.82 ± 0.15	0.11 ± 0.15	0.0025
	75	0.81 ± 0.70	0.0068 ± 0.00045	0.0023
	150	0.67 ± 0.070	0.0063 ± 0.00015	0.0023
	750	0.022 ± 0.0030	0.0043 ± 0.000064	0.0018
	Average	0.73 ± 0.16	0.086 ± 0.049	0.0022
4.95	7.5	0.92 ± 0.032	0.00037 ± 0.0023	0.0010
	15	1.02 ± 0.053	0.020 ± 0.0023	0.0015
	37.5	0.79 ± 0.038	0.011 ± 0.00029	0.0010
	75	0.85 ± 0.10	0.010 ± 0.000083	0.0015
	150	0.34 ± 0.020	0.0088 ± 0.000050	0.0020
	375	0.022 ± 0.00065	0.0051 ± 0.000091	0.0020
	1500	0.014 ± 0.00014	0.0033 ± 0.000028	0.0025
	Average	0.57 ± 0.035	0.0085 ± 0.00074	0.0017
10.00	7.5	1.12 ± 0.13	0.029 ± 0.011	0.0025

	15	0.76 ± 0.052	0.033 ± 0.0020	0.0025
	75	0.21 ± 0.012	0.021 ± 0.00019	0.0035
	150	0.069 ± 0.0026	0.015 ± 0.00019	0.0040
	750	0.043 ± 0.0012	0.011 ± 0.000078	0.0030
	Average	0.44 ± 0.040	0.022 ± 0.0026	0.0031
14.85	7.5	3.08 ± 1.44	0.11 ± 0.0030	0.0040
	15	1.13 ± 0.10	0.049 ± 0.0011	0.0060
	75	0.13 ± 0.0055	0.031 ± 0.00036	0.0030
	150	0.11 ± 0.0028	0.027 ± 0.00021	0.0040
	750	0.20 ± 0.053	0.031 ± 0.00039	0.010
	Average	0.93 ± 0.32	0.050 ± 0.0010	0.0054

Table S2. Summary of k_f values for 4.95 mM at 520 nm, for one step model (A \rightarrow B). As k_f values are inconsistent with each other, and correspond to poor residuals, a more complex (two-step) model is required for these data.

Time (s)	$k_{f-1step} (s^{-1})$	Residual
7.5	0.26 ± 0.0053	0.0015
15	0.065 ± 0.0020	-0.004 to 0.002, curved
37.5	0.017 ± 0.00042	Starts -0.008, then sharp increase to 0.002, then stays flat
75	0.011 ± 0.000086	Starts at -0.004, sharp increase to 0.0015, then flat
150	0.0096 ± 0.000071	Starts at -0.015, sharp increase to 0.002, then flat/slightly curved
375	0.0074 ± 0.000040	Starts -0.02 to 0.005, then dip and back to 0.005
1500	0.0062 ± 0.000055	Sharp increase from -.05 to 0.02, then dip and return to 0.01

Table S3. Summary of k_f values for two concentrations for two-step model ($A \rightarrow B \rightarrow C$) and the standard deviation for the residuals σ_r . For two Cu(I) concentrations, several timestamps were evaluated by stopped flow. The complete absorbance vs. time data were then imported into ReactLab KINETICS, in which the data evaluated under pseudo first-order kinetics with a global analysis. This was found to fit to a two-step model. See Table S4 for the corresponding data for a one step model. Please note, that the UV region is quite noisy in all measurements for sake of the 520 nm.

[Cu(I)] (mM)	Time (s)	k_{1-F} (s^{-1})	k_{2-F} (s^{-1})	σ_r
0.9	7.5	1.70 ± 0.08	0.24 ± 0.02	0.10
	15	1.02 ± 0.06	0.075 ± 0.03	0.10
	75	1.95 ± 0.03	0.0061 ± 0.0002	0.13
	150	1.73 ± 0.01	0.00674 ± 0.00009	0.14
	750	1.495 ± 0.0004	0.00660 ± 0.00003	0.17
[Cu(I)] (mM)	Time (s)	k_{1-F} (s^{-1})	k_{2-F} (s^{-1})	σ_r
10	7.5	1.6 ± 0.1	0.39 ± 0.03	0.25
	15	1.34 ± 0.01	0.21 ± 0.08	0.26
	75	0.93 ± 0.03	0.0296 ± 0.0005	0.27
	150	1.20 ± 0.04	0.0217 ± 0.0002	0.26
	750	1.41 ± 0.01	0.0134 ± 0.0001	0.27

Table S4. Summary of k_f values for two concentrations for global analysis and the standard deviation for the residuals σ_r , for one step model ($A \rightarrow B$). As k_f values are inconsistent with each other, a more complex (two-step) model is required for these data.

[Cu(I)] (mM)	Time (s)	k_{1-F} (s^{-1})	σ_r
0.9	7.5	0.115 ± 0.007	0.10
	15	0.114 ± 0.003	0.10
	75	0.0070 ± 0.0002	0.13
	150	0.00708 ± 0.00009	0.14
	750	0.00668 ± 0.00003	0.17
[Cu(I)] (mM)	Time (s)	k_{1-F} (s^{-1})	σ_r
10	7.5	0.21 ± 0.01	0.25
	15	0.137 ± 0.005	0.26
	75	0.0293 ± 0.0005	0.27
	150	0.0225 ± 0.0002	0.26
	750	0.0132 ± 0.0001	0.27

Table S5. Catalytic H₂Q oxidation to BQ by **T**_{OC4F9} in THF at -78°C.

[Cu ^I] [mM]	Cu ^I [equiv]	Initial H ₂ Q [equiv]	Final H ₂ Q [equiv]	Final BQ [equiv]	% Recovered (H ₂ Q + BQ)	TON
5.00 ^[a]	1.00	10.102	4.10	2.63	67.28%	7.90
5.00 ^[a]	1.00	9.989	4.18	3.78	48.19%	7.20
5.00 ^[a]	1.00	9.985	1.30	2.23	35.22%	6.65
5.00 ^[a]	1.00	10.00	2.19	2.19	43.86%	6.59
5.00 ^[a]	1.00	10.00	2.37	2.20	45.64%	6.59
5.00 ^[b]	1.00	10.00	1.74	2.00	37.45%	5.99
5.00 ^[b]	1.00	10.00	1.44	1.44	28.74%	4.31
5.00 ^[c]	1.00	10.00	2.69	2.69	53.81%	8.07
5.00 ^[c]	1.00	10.00	2.16	2.38	45.41%	7.14

[a] Catalytic reactions with **T**_{OC4F9} catalyzing conversion of H₂Q to BQ. Initial H₂Q based on Cu(I), and final H₂Q and BQ based on initial H₂Q, determined by quantitative ¹H NMR. TON based on **T**_{OC4F9}.

[b] Addition of sieves to catalytic reactions with **T**_{OC4F9} catalyzing conversion of H₂Q to BQ.

[c] Self-assembly reactions of **T**_{OC4F9} with H₂Q.

Table S6. Product quantification in hydroxylation of phenolate (DBP) to catecholate (DBC) by T_{OC4F9} in THF at $-78^{\circ}C$								
Run	[Cu] ^I [mM]	Cu ^I [equiv]	Initial DBP [equiv]	Final DBP [equiv]	Final DBC [equiv]	Total % Collected (Phenol+ Catechol)	%Conversion (based on 1 {Cu ₃ O ₂ } unit)	Product A or B, Shifts (ppm)
1	5.00	1.00	1.000	0.83	0.09	90.0	27	A (6.82, 6.73)
2	5.00	1.00	1.003	0.60	0.10	70.0	30	A (6.69, 6.79)
3	5.00	1.00	1.003	0.63	0.21	84.0	63	A (6.80, 6.69)
4	5.00	1.00	5.000	3.70	0.20	78.0	60	A (6.84, 6.75)
5	5.00	1.00	5.000	3.50	0.45	79.0	135	A (6.81, 7.72)
6	5.00	1.00	5.000	2.75	0.20	59.0	60	A (6.82, 6.74)
7	5.00	1.00	5.001	2.85	0.20	61.0	60	A (6.72, 6.84)
8	5.00	1.00	5.000	2.85	0.25	62.0	75	A (6.84, 6.76)
9	5.00	1.00	5.000	2.10	0.25	47.0	75	A (6.82, 6.74)
10	5.00	1.00	4.998	2.60	0.35	59.0	105	A (6.84, 6.76)
11	5.00	1.00	4.988	2.40	0.30	54.0	90	A (6.83, 6.74)
12	5.00	1.00	4.983	2.50	0.55	61.0	165	A (6.82, 6.76)
13	5.00	1.00	5.017	2.31	0.35	53.0	105	A (6.76, 6.61)
14	5.00	1.00	5.046	3.20	0.30	69.4	90	A (6.76, 6.61)
15	5.00	1.00	5.000	3.74	0.38	82.4	114	A (6.86, 6.79), and B (6.98, 6.21)
16	5.00	1.00	5.000	3.62	0.38	80.0	114	B (6.97, 6.21)
¹⁸ O	5.00	1.00	5.000	1.84	0.14	39.6	42	A (6.86, 6.78)
	Average (standard deviation) for 1 eq DBP			0.69± 0.10	0.13± 0.05	82.00± 9.09	40.00± 16.31	
	Average (standard deviation) for 5 eq DBP			2.93± 0.54	0.32± 0.10	64.98± 11.14	96.00± 30.30	